Published in final edited form as:
J Comp Neurol. 2014 June 15; 522(9): 2038–2052. doi:10.1002/cne.23515.

Invertebrate Specific D1-like Dopamine Receptor in Control of Salivary Glands in the Black-Legged Tick *Ixodes scapularis*

Ladislav Šimo, **Juraj Koči**, **Donghun Kim**, and **Yoonseong Park**
Department of Entomology, Kansas State University, Manhattan, KS 66506, USA

Abstract

The control of tick salivary secretion, which plays a crucial role in compromising the host immune system, involves complex neural mechanisms. Dopamine is known to be the most potent activator of salivary secretion, as a paracrine/autocrine factor. We describe the invertebrate specific D1-like dopamine receptor (InvD1L), which is highly expressed in tick salivary glands. The InvD1L phylogenic clade was found only in invertebrates, suggesting that this receptor was lost in the vertebrates during evolution. InvD1L expressed in CHO-K1 cells was activated by dopamine with a median effective dose (EC_{50}) of 1.34 μM. Immunohistochemistry using the antibody raised against InvD1L revealed two different types of immunoreactivities: basally located axon terminals that are colocalized with myoinhibitory peptide (MIP) and SIFamide neuropeptides, and longer axon-like processes that are positive only for the InvD1L antibody and extended to the apical parts of the acini. Both structures were closely associated with the myoepithelial cell, as visualized by beta-tubulin antibody, lining the acinar lumen in a web-like fashion. Subcellular localizations of InvD1L in the salivary gland suggest that InvD1L modulates the neuronal activities including MIP/SIFamide varicosities, and leads the contraction of myoepithelial cells and/or of the acinar valve to control the efflux of the luminal content. Combining the previously described D1 receptor with its putative function for activating an influx of fluid through the epithelial cells of acini, we propose that complex control of the tick salivary glands is mediated through two different dopamine receptors, D1 and InvD1L, for different downstream responses of the acinar cells.

Keywords

InvD1L; salivary gland acini; synganglion; GPCR; myoepithelial cell

Introduction

Ixodid ticks, a large group of hematophagous arthropods, are capable of feeding on vertebrate hosts for several days (4–15 days), depending on the species and life stage. The

Corresponding author: Yoonseong Park (ypark@ksu.edu), 123 Waters Hall, Department of Entomology, Kansas State University, Manhattan, KS 66506, USA.

Conflict of interest statement
The authors declare that they have no competing interests.

Role of authors
All authors had full access to all the data in the study and take responsibility for the integrity of the data and the accuracy of the data analysis. Study concept and design: LŠ, YP. Acquisition of data: LŠ, JK, DK. Analysis and interpretation of data: LŠ, JK, DK, YP. Writing the manuscript: LŠ, YP.

long-term feeding of the ticks is achieved by secretions of bioactive tick saliva that manipulate the host responses to their bite, and the saliva includes components that possess anti-hemostatic and immunomodulatory activities. An additional function of the salivary secretion is to remove excess water and ions from the large amount of ingested blood, thereby maintaining homeostasis (Kaufman and Phillips, 1973; Tatchell, 1967). Pathogen transmission also occurs through tick salivary secretion (Bowman et al., 1997; Bowman and Sauer, 2004; Ribeiro et al., 2006). The mechanisms controlling tick salivary secretion have been intensively studied over the last four decades.

The salivary gland (SG) of Ixodid ticks consists of numerous acini (also called alveoli) that form grape-like clusters on the lateral part of the body. Three different types of acini have been identified in female Ixodid ticks. Agranular type I acini are primarily attached on the main duct, and their size remains constant during tick feeding. In contrast, types II and III acini occupy the proximal and distal portions of the lobular duct branches, respectively, and they greatly increase in size during feeding and are thought to be the major producers of bioactive molecules and of excretory fluid during tick feeding (Binnington, 1978; Gaede et al., 1997; Rudolph and Knulle, 1974; Šimo et al., 2013).

Dopamine (DA) has been shown to be the most potent activator of SG secretion in both *in vitro* and *in vivo* experiments (Bowman and Sauer, 2004; Kaufman, 1976; Kaufman, 1978; Lees and Bowman, 2007). The search for the source of the endogenous DA in the tick uncovered a large amount of DA in the SG. This discovery led to the hypothesis that DA acts as the paracrine or autocrine controller of the SG itself (Kaufman et al., 1999; Šimo et al., 2011a also see review Kaufman, 2010), although DA is also well known for its major function as a neurotransmitter in the nervous systems of many animals.

Intracellular signal transduction in DA-induced salivary secretion has been investigated and identified as dependent on cyclic AMP (cAMP) and cAMP-dependent protein kinase (PKA, (Mane et al., 1985; Mane et al., 1988; Schmidt et al., 1981), which is a typical intracellular coupling of D1-type DA receptors (Hemmings et al., 1984). Likewise, exogenous cAMP stimulates fluid secretion in isolated tick SG (Needham and Sauer, 1979; Needman and Sauer, 1975). Interestingly, the DA-induced and cAMP-mediated salivary secretion required extracellular Ca^{++} (Needman nad Sauer 1979). Therefore, the DA signal transduction is thought to involve at least two different downstream pathways mediated by cAMP and Ca^{++}.

We previously identified the D1 receptor in the tick SG, and immunohistochemistry (IHC) suggested that the receptors are localized on the luminal surface of epithelial cell junctions in acini II and III. The D1 receptor was preferentially coupled with cAMP elevation in a heterologous expression, consistent with a part of it being a component of DA-mediated signal transduction for salivary secretion (Šimo et al., 2011a). However, there are gaps in the understanding of DA-mediated physiology in the SG, particularly the requirement of Ca^{++} for DA-induced salivary secretion.

In the present study, we have characterized another DA receptor expressed in tick SGs. This receptor, previously described as Isdop2 or D1-like receptor (Ejendal et al., 2012; Mayer et

al., 2011; Šimo et al., 2011a), is closely related to the D1 receptor in the phylogeny, but it belongs to a unique cluster that is specific to invertebrate taxa. Therefore, we have named this receptor the invertebrate specific D1-like DA receptor (InvD1L) and this cluster of receptors the *InvD1 subgroup*. Based on the subcellular localizations, we propose that the combinatory actions of the D1 and InvD1L receptors orchestrate salivary secretion in tick SGs.

2 Materials and methods

2.1 Tick samples and chemicals

Unfed adult *I. scapularis* ticks were obtained from a tick-rearing facility at Oklahoma State University. Approximately 25 male and 25 female individuals of *I. scapularis* were kept separately in polypropylene tubes (9 × 2.5 cm) with the openings covered by wet cotton plugs. Each vial contained a small piece of filter paper (4 × 1 cm). The tubes were kept in a dark, humid chamber at 4 °C. Tick feeding was performed on New Zealand White rabbits (Myrtle's Rabbitry, TN). The rabbits were cared for in accordance with the guidelines established by the Institutional Animal Care and Use Protocol (IACUC Approval No. 3050) of Kansas State University.

The following chemicals used in this study were purchased from Sigma-Aldrich (St. Louis, MO) unless otherwise specified: dopamine hydrochloride, DL-octopamine hydrochloride (Fluka), (+)-butaclamol, pilocarpine nitrate salt, (±)–norepinephrine (NE) (+)-bitartrate salt, serotonin hydrochloride, (±) octopamine hydrochloride, tyramine hydrochloride, methylergonovine maleate salt, (±)-2-amino 6,7-dihydroxy-1,2,3,4,-tetrahydro-naphthalene hydrobromide, *R*-(−)-Apomorphine hydrochloride hemihydrate, (±)-SKF-82958 hydrobromide, dopamine-3-O-sulfate, and dopamine-4-O-sulfate (NIMH Chemical Synthesis and Drug Supply Program, RTI International).

2.2 Gene cloning and sequence analysis

Gene prediction was based on BLAST searches of the *I. scapularis* genome sequence (www.vectorbase.org), which yielded a gene encoding putative *I. scapularis* invertebrate specific receptors (InvD1L). The query sequence was based on previous reports of the *Drosophila melanogaster* DA receptor Dmel\dopR2 (also known as DAMB, DOPR99B; Feng et al., 1996), which belongs to the *InvD1L subgroup* of receptors. The predicted full-length open reading frame (ORF) of InvD1L was amplified from the cDNA obtained from the SGs of mixed-feeding phases of females by polymerase chain reaction (PCR) using the forward primer 5′-GATGCCAGTTCCGGGCGA-3′ and reverse primer 5′-CGTCAGCGCTATAGGACGG-3′. The PCR product for InvD1L was inserted into the pGEM-T-easy vector (Promega, Madison, WI) and then sequenced.

For the phylogenetic analyses, putative translations were aligned using CLUSTAL (Thompson et al., 1994). Only the sequences in the ranges of putative transmembrane domains 1 to 7, which have relatively high levels of conserved sequences, were used for the construction of a tree with 500 bootstrapping in the MEGA5 software (Kumar et al., 2008). The tree generated from the unweighted pair group method with arithmetic mean (UPGMA) is shown in this study, which was also well supported by other methods, such as the

neighbor-joining, minimum-evolution, maximum likelihood and maximum parsimony methods.

2.3 Receptor functional assays

The full-length ORF of *invd1l* was inserted into the expression plasmids pcDNA3.1(+) (Invitrogen). Transient expression of InvD1L with the aequorin reporter (human cytoplasmic aequorin) (Vernon and Printen, 2002) in Chinese hamster ovary (CHO-K1) cells was used for the detection of increased luminescence upon activation of the receptor, leading to ligand-induced calcium mobilization (Park et al., 2002; Park et al., 2003).

Luminescence assays were performed in opaque 96-well microplates (Corning, Tewksbury, MA) using an Orion microplate luminometer (Berthold Detection Systems). The negative control consisted of cells transfected with only the reporter construct aequorin, which showed no response to DA. Various doses of DA and DA receptor agonists (10 μM final concentration) were plated in each well (50 μL total volume). The changes in luminescence were monitored for 20 s immediately after the injection of cells into the well (~15,000 cells in 50 μL). The luminescent response was integrated over time and normalized to the luminescence induced by 10 μM DA, which is the concentration that produced the largest response. The average luminescence of the multiple wells containing only buffer was considered the background level for the normalization. For measuring the antagonistic activity of pharmacological reagents, i.e., (+)-butaclamol, the cells were incubated with different concentrations of (+)-butaclamol for 15 min. Subsequently, the cells were treated with 10 μM DA, the dose inducing the highest response, and the 20 s luminescent response was measured.

2.4 Quantitative real-time reverse transcriptase-PCR (qRT-PCR)

Female ticks were dissected in ice-cold sterile phosphate buffered saline (PBS; 137 mM NaCl, 1.45 mM NaH_2PO_4, and 20.5 mM Na_2HPO_4; pH 7.2). Dissected organs were immediately frozen in tubes, placed on dry ice and stored at −80 °C until use. Tick samples included unfed, daily samples after the onset of feeding to 6-day fed, and replete (i.e., fed for 7–9 days). For tissue-specific qRT-PCR analyses, cDNAs from all of the different stages were pooled to ensure the detection of temporally fluctuating messages in each tissue. Total RNA was extracted using either Trizol (Invitrogen, Carlsbad, CA) followed by a Turbo DNAse treatment (Ambion, Carlsbad CA) or the RNeasy Plus Micro Kit (Qiagen, MD), which utilizes an on-column DNase treatment to obtain DNA-free RNA. Reverse transcription according to the manufacturer's oligo(dT)20-based protocol was followed by real-time PCR using SYBR premix Ex Taq (Takara Bio Inc., USA). All data presented are for at least three biological replicates unless otherwise specified in the figure captions.

Primers for the qRT-PCR assay using the forward primer 5′-TTCTTCTGCTTCGTGACCAT-3′ and the reverse primer 5′-AGTGATAGCCCAATAGCG-3′ amplified a 277-bp-long fragment for InvD1L. The 80-bp-long amplicon encoding ribosomal protein S4 (GenBank Accession No. DQ066214) served as a reference gene, as described in previous studies (Koči et al., 2013; Šimo et al., 2013). The amplicons in the qRT-PCR were verified by melting curves and electrophoresis

on a 1.5% agarose gel to ensure the absence of primer-dimer formations and the specificity of the amplicons. Mean Ct values for the reference and target genes were generated from technical duplicates and used to calculate ΔΔCt values (Livak and Schmittgen, 2001). Fold differences in the expression of target genes in tissue-specific and stage-specific sample sets were deduced from a calibrated sample assigned the value of 1. Statistics on the mean ± SD were performed on at least three biological replicates using a one-way Student t-test ($P \leq 0.05$) in Origin v7 software (Northampton, MA).

2.5 Antibodies and immunohistochemistry

An affinity-purified antibody against InvD1L was raised in chickens (Genescript, New Jersey). An antigenic peptide for InvD1L was designed for the region that was predicted to have a high surface probability, high antigenicity and a low probability of post-translational modification. The 20 carboxy-terminal amino acid residues (CRIIKEDASMRSQSLEEAVL) were chemically synthesized and conjugated to keyhole limpet hemocyanin using the cysteine at the N-terminus of the peptide (Table 1.).

The antibody for the SIFamide neuropeptide has previously been described (Šimo et al., 2009b). The antibody recognized only neuronal cell bodies in the *I. scapularis* synganglion and their projections to visceral organs. Representative cells stained by these antibodies generally coincided with *in situ* hybridization for their respective mRNAs (Šimo et al., 2009b). Myoepithelial cells in SG acini were immunostained using an affinity-purified monoclonal anti-mouse antibody against whole human β-tubulin protein (Genescript, Table 1).

For whole-mount IHC of tick synganglia and SGs, we followed a previously established procedure (Šimo et al., 2009a, 2009b). Samples fixed in Bouin's solution were washed in PBS containing 1% Triton X-100 (PBST). For InvD1L receptor, MIP, SIFamide or myoepithelial cell (in the case of only SGs) staining, synganglia and SGs were subsequently incubated with the appropriate antibody or a mixture of antibodies. Dilutions for all primary and secondary antibodies were 1:1000. The secondary antibodies used in the study were as follows: Alexa 594, 647, and 488-goat anti-rabbit IgG, Alexa 594, and 488- goat anti-mouse IgG, and Alexa 594 or 488-goat anti-chicken IgG (Molecular Probes, Carlsbad, CA). Nuclei were stained with 300 nM 4′,6′-diamino-2-phenylindole (DAPI, Sigma). Images were acquired using a confocal microscope (Zeiss LSM 700). Image enhancements, i.e., alterations in contrast and brightness, were performed in Adobe Photoshop 7.0.

2.6 The nomenclature of peptidergic neurons

For the naming of peptidergic neurons, we followed a nomenclature system previously used for the hard tick *R. appendiculatus* (Šimo et al., 2009a). The first two letters of each name refer to the position of each neuron in a specific lobe/region of the synganglion, specifically cheliceral (Ch), prothocerebral (Pc), pedal 1–4 ($Pd_{1–4}$), opisthosomal (Os), or postesophageal (Po). The letters that follow the first two letters of each name refer to the anatomical location of the neuron, specifically dorsal (D), ventral (V), anterior (A), posterior (P), medial (M) or lateral (L). Neurons that innervate the acini of the salivary glands were labeled as SG.

3 Results

3.1 Phylogeny of InvD1L

The full-length ORF of the InvD1L was found to be intronless, encoding 457 amino acid residues and containing the typical GPCR signature of seven putative transmembrane domains. Comprehensive BLAST searches followed by phylogenetic analyses of the DA receptor revealed the orthologous cluster of InvD1L DA receptors (Fig. 1A). The InvD1L orthologues were found in the genomes of the species belong to the phyla/subphyla Hexapoda, Annelida, Chelicerata, Crustacea, Mollusca, Nematoda, Hemichordata, Echinodermata, Platyhelminthes, and Cephalochordata, but not in Vertebrata. Based on sequence similarity, surprisingly, the sister taxa of InvD1L was found to be the alpha-1 adrenergic receptors (ADRA1) cluster, which are absent in Insecta (Fig. 1A and B). Independent losses of the ADRA1 may also have occurred in Nematoda and Platyhelminthes based on currently available sequence information. The previously characterized *I. scapularis* D1 receptor (Meyer et al., 2011; Šimo et al., 2011a) belongs to the *D1 subgroup* of DA receptors and showed clear orthologous clustering with *Drosophila* DopR and the *H. sapiens* D1 and D5 receptors belonging to the clade, which was found in both invertebrate and vertebrate taxa (Fig. 1A). The *I. scapularis* genome also contains a gene encoding a D2 receptor that is in the orthologous cluster with *Drosophila* D2R and *H. sapiens* receptors D2, D3, and D4, (Fig. 1A; (Šimo et al., 2011a). In summary, we conclude that reciprocal losses of the ancestral sister group InvD1L and ADRA1 in vertebrates and insects, respectively, resulted in insects carrying only InvD1L. Because the naming conventions of the DA receptors are complex and confusing, we provide a table (Fig. 1C) that summarizes the nomenclature of the *Ixodes* and *Drosophila* DA receptors. GenBank Accession Numbers of the sequences for this analysis are in the Fig. 1 legend.

3.2 InvD1L ligand specificity

The aequorin reporter system measuring intracellular calcium mobilization upon activation of InvD1L showed significant responses only to DA (in the 30 nM to 60 μM range, EC_{50} value of 1.34 μM) and 10 μM 6,7-ADTN (known as a DA agonist) among the different drugs tested at various doses (Fig. 2A to C). Pre-treatment (15 minutes) with different concentrations (in the 10 nM to 60 μM range) of (+)butaclamol, a general DA receptor antagonist, showed suppression of DA (10 μM) mediated InvD1L activity with an EC_{50} value of 0.64 μM (Fig. 2D and E). Mock transfected cells, containing only the reporter aequorin, showed no activity in response to 10 μM DA.

3.3 Tissue- and stage-specific *invd1l* transcript

The tissue-specific qRT-PCR revealed the presence of *invd1l* transcripts in synganglia and SGs in the pooled samples of multiple feeding phases, unfed and 1- to 6-day fed, and replete females, while it was undetected from the carcasses (mixed sample of integument and all internal organs except SGs and synganglia; Fig. 3A). Further examination of the *invd1l* transcripts from different feeding phases of *Ixodes* females showed that the *invd1l* receptor mRNA was constitutively presented in the synganglia and SGs from pre-blood feeding to repletion. In synganglia, the *invd1l* transcript was significantly increased on the second day of feeding (2.5-fold), while the level fluctuated between ~0.15 to 1-fold over the feeding

phase (Fig. 3B). In the SGs, the *invd1l* transcript levels fluctuated between ~0.2 to 1-fold over the entire feeding period, with the highest abundance in unfed females, which were used for normalization (Fig. 3B).

3.4 Immunohistochemical localization of InvD1L in synganglia and salivary glands

The specificity of anti-InvD1L was confirmed by several control experiments. The negative controls were immunohistochemistry with pre-immune serum or with antibody preadsorbed with synthetic immunogenic peptide (Fig. 4A–C). The antibody specificity was also characterized by positive signals in CHO-K1 cells transfected with *invd1l* and by a lack of immunoreactivity (IR) in cells incubated with the respective pre-immune serum or in mock transfected cells (Fig. 4D–E). In addition, the BLAST search of the *I. scapularis* genome using the antigenic peptide sequence as a query did not reveal any significant matches, except to the InvD1L receptor gene.

IHC of InvD1L revealed different clusters of neurons in various regions of synganglia. A total of 28 pairs of neurons were detected in both the dorsal and ventral sides of the protocerebrum: PcAM, $PcDM_{1-6}$, $PcDL_{1-9}$, PcDM, PcSG, $PcDP_{1-4}$, $PcVM_{1-4}$, and PcVL (Figs. 5A, 6). The most prominent large pair of protocerebral neurons (PcSG) having axonal projections to the SG acini II and III (Šimo et al., 2009b) showed coexpression of InvD1L and two neuropeptides, MIP and SIFamide (Fig. 5C). Multiple InvD1L immunoreactive neurons were also observed in different regions of all four pedal ganglia (20 pairs: Pd_1DL_{1-5}, Pd_2DL, Pd_3DM, $Pd_4DM_{1,2}$, Pd_1VL, and $Pd_{1-4}VM_{1-10}$), opisthosomal ganglia (12 pairs: OsDM, $OsDM_{1-7}$, and OsVM1-4), and one pair of neurons in the postesophageal region (PoAM) (Fig. 5).

Two different types of InvD1L IRs were revealed in both acini II and III in the IHC for InvD1L in SG (Fig. 5D,E, 7). The most obvious and consistent IR was observed in 3–4 and 4–5 axon terminals, reaching the basal regions of SG acini II and III, respectively (Fig. 5D,E, 7, 8). InvD1L axonal projections, innervating SGs, showed exactly the same staining pattern as previously described for colocalization of MIP and SIFamide neuropeptides (Fig. 7; Šimo et al., 2009b). The origin of these axon terminals is likely the pair of protocerebral neurons (PcSG) that are also immunoreactive for InvD1L and both MIP and SIFamide neuropeptides (Fig. 5C, 8). The InvD1L/MIP/SIFamide-IRs exit the synganglion through salivary nerve 1 (a branch of the palpal nerve), run along the main salivary duct, and enter acini II and III in their neck regions, where they arborize into their basal parts close to the lumen (Fig. 8). The IR was observed in unfed, daily collected samples of 1- to 6-day fed, and replete females, indicating a constitutive presence of InvD1L in axon terminals. The lengths of the InvD1L axon terminals in the type II acini slightly increased from ~25 μm in the unfed samples to ~50 μm in the later stages (4–6 day) of feeding, while the length of the axon terminals in the type III acini remained constant at ~25 μm and was limited to the basal region.

Another type of InvD1L-IR observed in the SG acini was longer axon-like processes that extended to the apical regions of acini types II and III (Figs. 4D, E, 6A to I, 7). The axon-like structures enter each acinus (types II and III) through the basal region, arborize close to the lumen in 5–7 branches, and terminate in the apical region of the acini. The InvD1L-IR

axon-like processes are distinguished from the InvD1L/MIP/SIFamide-IR axons by their longer projections and by the IR to only InvD1L antibody and not to MIP or SIFamide antibodies. The cellular source of the InvD1L-IR axon-like processes was unidentified, despite extensive IHC efforts on large numbers of SGs in various feeding phases. We also investigated whether the longer axon-like IR processes are the same as those we previously described for IR to anti-pigment dispersing factor (anti-PDF) that appeared exclusively in type II acini (Šimo et al., 2009a; also see review Šimo et al., 2011b). However, double-staining showed that the InvD1L-IR is different from the PDF-IR in these types of acini (data not shown).

In unfed females, the length of these IR axon-like processes is ~45 μm for both type II and III acini, and almost the entire length of an acinus in this particular stage. During feeding, the length of the IR axon-like processes in the type II acini slightly increased to ~60 μm in the later stages, whereas the IR in the type III acini completely disappeared within the first 2 days after the initiation of feeding (Fig. 7J and L). In most of the samples tested (>100 SGs), the IRs were detected within the acini, originating from the neck region, with the process reaching the apical region. In rare occasions, however, the basal extensions of the IR processes were detectable on the salivary ducts, along with InvD1L/MIP/SIFamide-IR axons near the neck regions of types II and III acini (Fig. 5C).

We used various antibodies for immunohistochemical stainings to understand the cellular and subcellular structures of the acini. We found that β-tubulin IR revealed a single myoepithelial cell (Krolak et al., 1982) in types II and III acini (Fig. 7). The web-like luminal β-tubulin IR in the junctions between epithelial cells in unfed ticks is clearly consistent with myoepithelial cell previously described in electron microscopy studies (Coons et al., 1994; Krolak et al., 1982). The β-tubulin-IR changed after feeding, along with the increased size of the acini. In type II acini from 4-day fed ticks, the fine, thread-like β-tubulin-IR is further dispersed to the edges of the acini. We are uncertain whether this change in β-tubulin-IR is caused by the morphological changes of the myoepithelial cell or by the changes in other cell types that may express β-tubulin in the later stage of feeding. The β-tubulin-IR became considerably weaker after feeding in type III acini (Fig. 7), while a narrow, web-like network of myoepithelial cell remains in ultrastructural observations (Koči and Park, unpublished data). In triple staining with InvD1L, SIFamide and β-tubulin antibodies, we found a close association of InvD1L-IRs with myoepithelial cells in both type II and III acini. The basally located InvD1L/MIP/SIFamide-IR axon terminals, originating from PcSG neurons, are closely associated with the basal part of the myoepithelial cell, surrounding the acinar duct and its valve. In contrast, the longer InvD1L-IR axon-like processes in type II acini (all feeding stages) and type III acini (only unfed stage and 1–2 days fed) surround the entire luminal region, including the apical part of the myoepithelial cell (Fig. 7, 8). We conclude from the current optical resolution that the longer InvD1L axon-like processes are either subcellular structures of myoepithelial cell or independent axonal processes.

Discussion

Tick salivary secretion likely involves complex neural control. It has been shown to involve various neuropeptide molecules delivered via axonal projections to different regions of SG (Šimo et al., 2009a, 2009b; Šimo et al., 2011b; Šimo et al., 2013). Among those, the two neuropeptides myoinhibitory peptide (MIP) and SIFamide, along with their receptors, were investigated in detail in our previous reports (Šimo et al., 2013).

Downstream of the neural commands, paracrine or autocrine DA in the SG directly activates the salivary secretion, as described in numerous studies (Kaufman, 1978; Kaufman and Wong, 1983; Schmidt et al., 1981; Šimo et al., 2011a; also see reviews Bowman and Sauer, 2004; Lees and Bowman, 2007). In our recent study, we showed that the D1 receptor is expressed in the epithelial cells of SG acini II and III, which are presumed to mediate the activation of the influx of fluid into acini (Šimo et al., 2011a). In the present study, we describe another DA receptor, InvD1L, which is also expressed in the SG acini and likely plays different roles in salivary secretion. The InvD1 was previously described as Ixodop2 or D1-like receptor (Ejendal et al., 2012; Mayer et al., 2011; Šimo et al., 2011a)

In-depth phylogenetic analysis of the *InvD1 subgroup* indicates that the sister clade of InvD1L is that of the adrenergic receptor ADRA1, while D1 receptors of insects and vertebrates are in further diverged clades and thus form the immediate outgroup. The divergence between ADRA1 and InvD1L may have occurred at the ancestral lineage of Bilataria before the divergence of Deuterostomia and Protostomia, while the loss of InvD1L in vertebrates and the loss of ADRA1 in insect subsequently occurred.

Ligand specificities of InvD1L and ADRA1 also indicate that functional divergence of the receptors specific to DA and adrenaline, respectively, has been established. In our study, the InvD1L of *I. scapularis* was activated by DA but was not responsive to norepinephrine (10 μM). Previous studies in *D. melanogaster* indicated that DA is the most potent activator of InvD1L (called Dmel\dopR2 in *Drosophila*), whereas epinephrine and norepinephrine had ~10 times lower activities (Feng et al., 1996). A later study on the *Drosophila* InvD1L receptor also showed that norepinephrine is 100 times less potent than DA (Han et al., 1996). At the same time, the ADRA1 is known to be activated preferentially by adrenergic ligands such as epinephrine or norepinephrine, while DA showed lower activities in both *in vivo* and *in vitro* experiments (Schmitz et al., 1981; Schwinn et al., 1990). The studies showing ligand specificities of InvD1L and ADRA1 are limited to the cases of insects and mammals, which happen to have lost the ADRA1 and InvD1L, respectively. Therefore, conclusions about the functional divergence of those receptors await data from the taxa carrying both receptors.

In the heterologous expression system, the downstream intracellular signaling cascade for InvD1L was linked to Ca^{++} mobilization but not to cAMP elevation. In contrast, Meyer et al. (2011) reported cAMP accumulation downstream of InvD1L (*Is*Dop2), but without testing Ca^{++} mobilization. This discrepancy may be caused by the use of different assay methods. Specifically, we speculate that the reporter assay using cAMP responsive element-luciferase (CRE-Luc), requiring a long incubation time with the ligand, may have caused

accumulation of cAMP by Ca^{++}-mediated indirect effects in the earlier study. Interestingly, the sister group of receptors ADRA1 is also known to activate Ca^{++} mobilization (Chen and Minneman, 2005). In our previous study, the D1 receptor was preferentially coupled with cAMP elevation, while it also resulted in Ca^{++} mobilization at higher concentrations of DA (Šimo et al., 2011a). Together with our previous study, we propose that the InvD1L is coupled with Ca^{++} mobilization, whereas the D1 receptor is preferentially coupled with cAMP elevation. Likewise, earlier studies have shown the requirement of two different intracellular signal transduction pathways, mediated by cAMP and Ca^{++}, in DA-mediated tick salivary secretion (Bowman et al., 1995; Schmidt et al., 1981; also see review Sauer et al., 2000). It remains to investigate whether the hypothetical downstream cellular signaling occurs in the specific cell types in the acini.

The *InvD1L* transcript was present in all feeding phases, in both SGs and synganglia based on the qRT-PCR. We could not identify the cellular source of the *InvD1L* transcript in the SGs because *in situ* hybridization did not reveal any cell bodies in the SGs (data not shown). Axonal transport of mRNA followed by protein synthesis in the axonal domains in invertebrates has been described (see review Mohr and Richter 2000). Therefore, the InvD1L mRNA in the SG could be the transcript delivered from off-SG cells (neurons) or in unidentified cells in the SG.

The basally located InvD1L/MIP/SIFamide axon terminal suggests that the DA in the SGs has a neuromodulatory function through the InvD1L as a means of feedback control on the peptidergic neuron. A previous TEM study of SG acini described the axons with large dense-core vesicles, typical vesicles containing neuropeptides, located near and through the basal part of myoepithelial cell (Krolak et al., 1982). Although the specific roles of MIP and SIFamide in tick SG acini remain unknown, three types of potential target cells were recently proposed based on the location of SIFamide receptor expression: myoepithelial cell, which may function in the contraction of the acini and/or the control of the valve; large, basally located dopaminergic granular cells for regulation of paracrine DA; and neck cells that may be involved in the control of the acinar duct and its valve (Šimo et al., 2013). Therefore, InvD1L is proposed as the modulator of the neuropeptidergic control of SGs.

The longer axon-like InvD1L-IR processes reach the apical parts of type II and III acini. Although further research is ongoing, we provide three possible hypotheses for the structure newly identified by InvD1L-IR: 1) The InvD1L-IR is a projection from a neuronal cell that remains to be identified; 2) InvD1L-IR is a subcellular structure of a myoepithelial cell, not a neural process; or 3) the InvD1L-IR is the terminal extensions of a basally located InvD1/MIP/SIFamide-IR axon and thus originates from central PcSG neurons. Although we prefer the first hypothesis of the InvD1L-IR as a neuronal projection by the appearance of the staining pattern showing like an axon terminal, a conclusion requires further ultrastructural study. Regardless of the cellular nature of the InvD1L-IR, the close association of these processes with myoepithelial cells implies that they function in mediating the control of the myoactivity of acini (Coons et al., 1994).

The myoepithelial cell, also named the adluminal cell or Cap cell (Krolak et al., 1982; Meredith and Kaufman, 1973), lines the luminal surface of acini, as shown by the strong β-

tubulin-IR in this study (Fig. 7). Myoepithelial cell has been proposed to function through pulsatile contractions of the acinus for expelling the acinar contents to the associated duct (Coons et al., 1994; Coons and Roshdy, 1973), though the luminal location of myoepithelial cells in tick SG is the opposite of the similar system in mammalian glandular organs, in which myoepithelial cells are located on the basolateral surface of luminal secretory cells (Adriance et al., 2005; Ogawa, 2003). In addition, the β-tubulin-IR extended to the neck region of acini (Fig. 7), supporting the previous ultrastructural study that showed the extended myoepithelial cell surrounding the acinar valve (Krolak et al., 1982). Therefore, the function of myoepithelial cell may be both for acinar contraction and control of the acinar valve.

In conclusion, tick SGs using paracrine DA as the signal for salivary secretion contains at least two different DA receptors, D1 and InvD1L. The divergent actions of the receptors discussed in this study may depend on the differences in sensitivities of the receptors and downstream cellular signals. InvD1 showed lower sensitivity to DA than did D1. In addition, in our assays, InvD1 is preferentially coupled with Ca^{++} mobilization but not with cAMP elevation. Finally, the InvD1L-IR in the neuropeptidergic axon terminals indicates that it is likely involved in the modulation of MIP/SIFamide signals. The InvD1L-IR in longer axon-like processes associated with myoepithelial cell suggests that the InvD1L is also involved in the control of the myoepithelial cell for acinar contraction and/or control of the acinar valve.

Supplementary Material

Refer to Web version on PubMed Central for supplementary material.

Acknowledgments

We gratefully thank to Dr. Jan Veenstra for providing the SIFamide antibody. This paper is contribution no. 14-016-J from the Kansas Agricultural Experiment Station and was supported by National institute of health; Grant Number: R01AI090062.

Abbrevations

ADRA1	alpha-1 adrenergic receptor
InvD1L	invertebrate specific D1-like dopamine receptor
MIP	myoinhibitory peptide
OsDM	opistosomal dorsomedial neuron
OsVM	opistosomal ventromedial neuron
PaN	palpal nerve
PcAM	protocerebral anteromedial neuron
PcDL	protocerebral dorsolateral neuron
PcDM	protocerebral dorsomedial neuron

PcDP	protocerabral dorso-posterior neuron
PcSG	protocerebral neurons innervating salivary glands
PcVL	protocerebral ventrolateral neuron
PcVM	protocerebral ventromedial neuron
PdDL	pedal dorsolateral neuron
PdDM	pedal dorsomedial neuron
PdVL	pedal ventrolateral neuron
PdVM	pedal ventromedial neuron
SgN	salivary nerve

Literature cited

Adriance MC, Inman JL, Petersen OW, Bissell MJ. Myoepithelial cells: good fences make good neighbors. Breast Cancer Res. 2005; 7(5):190–197. [PubMed: 16168137]

Binnington KC. Sequential changes in salivary gland structure during attachment and feeding of the cattle tick, *Boophilus microplus*. International journal for parasitology. 1978; 8(2):97–115. [PubMed: 681074]

Bowman AS, Coons LB, Needham GR, Sauer JR. Tick saliva: recent advances and implications for vector competence. Medical and veterinary entomology. 1997; 11(3):277–285. [PubMed: 9330260]

Bowman AS, Dillwith JW, Madden RD, Sauer JR. Regulation of free arachidonic acid levels in isolated salivary glands from the lone star tick: a role for dopamine. Archives of insect biochemistry and physiology. 1995; 29(3):309–327. [PubMed: 7655056]

Bowman AS, Sauer JR. Tick salivary glands: function, physiology and future. Parasitology. 2004; 129(Suppl):S67–81. [PubMed: 15938505]

Chen ZJ, Minneman KP. Recent progress in alpha1-adrenergic receptor research. Acta pharmacologica Sinica. 2005; 26(11):1281–1287. [PubMed: 16225747]

Coons LB, Lessman CA, Ward MW, Berg RH, Lamoreaux WJ. Evidence of a myoepithelial cell in tick salivary glands. International journal for parasitology. 1994; 24(4):551–562. [PubMed: 8082985]

Coons LB, Roshdy MA. Fine structure of the salivary glands of unfed male *Dermacentor variabilis* (Say) (Ixodoidea: Ixodidae). The Journal of parasitology. 1973; 59(5):900–912. [PubMed: 4744522]

Ejendal KF, Meyer JM, Brust TF, Avramova LV, Hill CA, Watts VJ. Discovery of antagonists of tick dopamine receptors via chemical library screening and comparative pharmacological analyses. Insect biochemistry and molecular biology. 2012; 42(11):846–53. [PubMed: 23213654]

Feng G, Hannan F, Reale V, Hon YY, Kousky CT, Evans PD, Hall LM. Cloning and functional characterization of a novel dopamine receptor from *Drosophila melanogaster*. J Neurosci. 1996; 16(12):3925–3933. [PubMed: 8656286]

Gaede K, Knülle W. On the mechanism of water vapour sorption from unsaturated atmospheres by ticks. The Journal of experimental biology. 1997; 200(Pt 10):1491–1498. [PubMed: 9319391]

Han KA, Millar NS, Grotewiel MS, Davis RL. DAMB, a novel dopamine receptor expressed specifically in *Drosophila* mushroom bodies. Neuron. 1996; 16(6):1127–1135. [PubMed: 8663989]

Hemmings HC Jr, Greengard P, Tung HY, Cohen P. DARPP-32, a dopamine-regulated neuronal phosphoprotein, is a potent inhibitor of protein phosphatase-1. Nature. 1984; 310(5977):503–505. [PubMed: 6087160]

Kaufman W. The influence of various factors on fluid secretion by in vitro salivary glands of ixodid Ticks. The Journal of experimental biology. 1976; 64(3):727–742. [PubMed: 180228]

Kaufman WR. Actions of some transmitters and their antagonists on salivary secretion in a tick. The American journal of physiology. 1978; 235(1):R76–81. [PubMed: 677342]

Kaufman WR. Ticks: physiological aspects with implications for pathogen transmission. Ticks and tick-borne diseases. 2010; 1(1):11–22. [PubMed: 21771507]

Kaufman WR, Phillips JE. Ion and water balance in the Ixodid tick Dermacentor andersoni I Routes of ion and water excretion. Journal of Experimental Biology. 1973; (58):523–536. [PubMed: 4765348]

Kaufman WR, Sloley DB, Tatchell RJ, Zbitnew GL, Diefenbach TJ, Goldberg JI. Quantification and cellular localization of dopamine in the salivary gland of the ixodid tick *Amblyomma hebraeum*. Experimental & Applied Acarology. 1999; 23:251–256.

Kaufman WR, Wong DL. Evidence for multiple receptors mediating fluid secretion in salivary glands of ticks. European journal of pharmacology. 1983; 87(1):43–52. [PubMed: 6188618]

Koči J, Šimo L, Park Y. Validation of internal reference genes for real-time quantitative polymerase chain reaction studies in the tick, *Ixodes scapularis* (Acari: Ixodidae). Journal of medical entomology. 2013; 50(1):79–84. [PubMed: 23427655]

Krolak JM, Ownby CL, Sauer JR. Alveolar structure of salivary glands of the lone star tick, *Amblyomma americanum* (L.): unfed females. The Journal of parasitology. 1982; 68(1):61–82. [PubMed: 7200514]

Kim YJ, Žitňan D, Cho KH, Schooley DA, Mizoguchi A, Adams ME. Central peptidergic ensembles associated with organization of an innate behavior. Proc Natl Acad Sci U S A. 2006; 103:14211–14216. [PubMed: 16968777]

Kumar S, Dudley J, Nei M, Tamura K. MEGA: a biologist-centric software for evolutionary analysis of DNA and protein sequences. Brief Bioinform. 2008; 9:299–306. [PubMed: 18417537]

Lees K, Bowman AS. Tick neurobiology: recent advances and the post-genomic era. Invert Neurosci. 2007; 7(4):183–198. [PubMed: 17962985]

Livak KJ, Schmittgen TD. Analysis of relative gene expression data using real-time quantitative PCR and the 2(−Delta Delta C(T) Method. Methods. 2001; 25(4):402–408. [PubMed: 11846609]

Mane SD, Darville RG, Sauer JR, Essenberg RC. Cyclic AMP-dependent protein kinase from the salivary glands of the tick, *Amblyomma americanum* partial purification and properties. Insect Biochem. 1985; 15:777–787.

Mane SD, Sauer JR, Essenberg RC. Molecular forms and free cAMP receptors of the cAMP-dependent protein kinase from tick salivary glands. Compo Biochem Compo Biochem Physiol. 1988; 9 IB:117–124.

Meredith J, Kaufman WR. A proposed site of fluid secretion in the salivary gland of the ixodid tick *Dermacentor andersoni*. Parasitology. 1973; 67:205–217. [PubMed: 4127146]

Meyer JM, Ejendal KF, Watts VJ, Hill CA. Molecular and pharmacological characterization of two D(1)-like dopamine receptors in the Lyme disease vector, Ixodes scapularis. Insect biochemistry and molecular biology. 2011; 41(8):563–571. [PubMed: 21457782]

Mohr E, Richter D. Axonal mRNAs: functional significance in vertebrates and invertebrates. J Neurocytol. 2000; 29(11–12):783–91. [PubMed: 11466470]

Needham GR, Sauer JR. Involvement of calcium and cyclic AMP in controlling ixodid tick salivary fluid secretion. Journal of Parasitology. 1979; 65:531–542. [PubMed: 229203]

Needman G, Sauer J. Control of fluid secretion by isolated salivary glands of the Lone Star tick. J Insect Physiol. 1975; 21:1893–1898. [PubMed: 1194704]

Ogawa Y. Immunocytochemistry of myoepithelial cells in the salivary glands. Progress in histochemistry and cytochemistry. 2003; 38(4):343–426. [PubMed: 14509196]

Park Y, Kim YJ, Adams ME. Identification of G protein-coupled receptors for Drosophila PRXamide peptides, CCAP, corazonin, and AKH supports a theory of ligand-receptor coevolution. Proc Natl Acad Sci U S A. 2002; 99(17):11423–11428. [PubMed: 12177421]

Park Y, Kim YJ, Dupriez V, Adams ME. Two subtypes of ecdysis-triggering hormone receptor in *Drosophila melanogaster*. J Biol Chem. 2003; 278(20):17710–17715. [PubMed: 12586820]

Ribeiro JM, Alarcon-Chaidez F, Francischetti IM, Mans BJ, Mather TN, Valenzuela JG, Wikel SK. An annotated catalog of salivary gland transcripts from Ixodes scapularis ticks. Insect biochemistry and molecular biology. 2006; 36(2):111–129. [PubMed: 16431279]

Rudolph D, Knulle W. Site and mechanism of water vapour uptake from the atmosphere in ixodid ticks. Nature. 1974; 249(452):84–85. [PubMed: 4833236]

Sauer JR, Essenberg RC, Bowman AS. Salivary glands in ixodid ticks: control and mechanism of secretion. Journal of insect physiology. 2000; 46(7):1069–1078. [PubMed: 10817833]

Schmidt SP, Essenberg RC, Sauer JR. Evidence for a D1 dopamine receptor in the salivary glands of Amblyomma americanum (L.). Journal of cyclic nucleotide research. 1981; 7(6):375–384. [PubMed: 7346526]

Schmitz JM, Graham RM, Sagalowsky A, Pettinger WA. Renal alpha-1 and alpha-2 adrenergic receptors: biochemical and pharmacological correlations. The Journal of pharmacology and experimental therapeutics. 1981; 219(2):400–406. [PubMed: 6270306]

Schwinn DA, Lomasney JW, Lorenz W, Szklut PJ, Fremeau RT Jr, Yang-Feng TL, Caron MG, Lefkowitz RJ, Cotecchia S. Molecular cloning and expression of the cDNA for a novel alpha 1-adrenergic receptor subtype. The Journal of biological chemistry. 1990; 265(14):8183–8189. [PubMed: 1970822]

Šimo L, Koči J, Park Y. Receptors for the neuropeptides, myoinhibitory peptide and SIFamide, in control of the salivary glands of the blacklegged tick *Ixodes scapularis*. Insect biochemistry and molecular biology. 2013; 43(4):376–387. [PubMed: 23357681]

Šimo L, Koči J, Žitňan D, Park Y. Evidence for D1 dopamine receptor activation by a paracrine signal of dopamine in tick salivary glands. PloS one. 2011a; 6(1):e16158. [PubMed: 21297964]

Šimo L, Slovák M, Park Y, Žitňan D. Identification of a complex peptidergic neuroendocrine network in the hard tick, *Rhipicephalus appendiculatus*. Cell Tissue Res. 2009a; 335(3):639–655. [PubMed: 19082627]

Šimo L, Žitňan D, Park Y. Neural control of salivary glands in ixodid ticks. Journal of insect physiology. 2011b; 58(4):459–466. [PubMed: 22119563]

Šimo L, Žitňan D, Park Y. Two novel neuropeptides in innervation of the salivary glands of the black-legged tick, *Ixodes scapularis*: myoinhibitory peptide and SIFamide. J Comp Neurol. 2009b; 517(5):551–563. [PubMed: 19824085]

Tatchell RJ. A modified method for obtaining tick oral secretion. The Journal of parasitology. 1967; 53(5):1106–1107. [PubMed: 6062065]

Terhzaz S, Rosay P, Goodwin SF, Veenstra JA. The neuropeptide SIFamide modulates sexual behavior in *Drosophila*. Biochem Biophys Res Commun. 2007; 352:305–310. [PubMed: 17126293]

Thompson JD, Higgins DG, Gibson TJ. CLUSTAL W: improving the sensitivity of progressive multiple sequence alignment through sequence weighting, position-specific gap penalties and weight matrix choice. Nucleic acids research. 1994; 22(22):4673–4680. [PubMed: 7984417]

Vernon WI, Printen JA. Assay for intracellular calcium using a codon-optimized aequorin. Biotechniques. 2002; 33(4):730, 732, 734. [PubMed: 12398176]

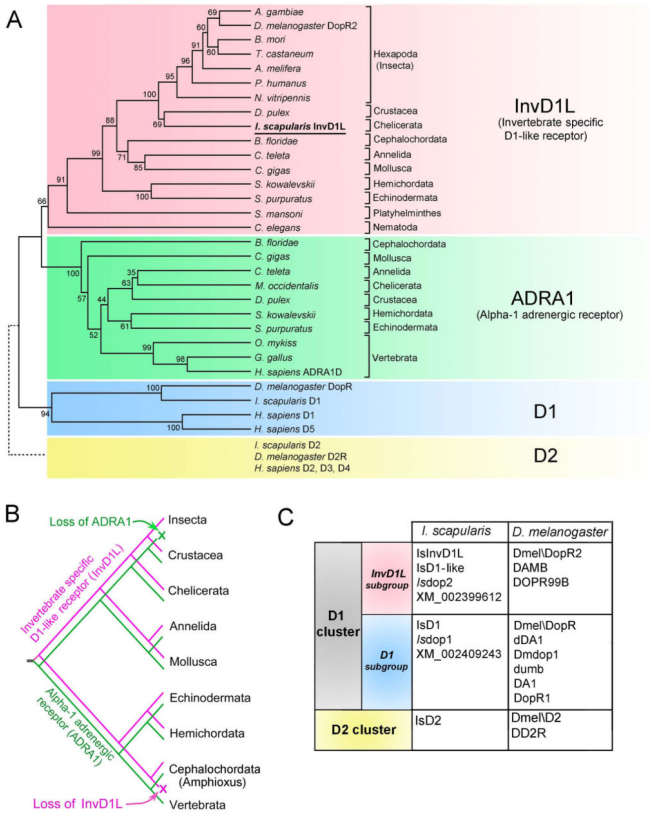

Figure 1.

Phylogeny of invertebrate specific D1-like receptor (InvD1L) and its sister clade, alpha-1 adrenergic receptor (ADRA1). (A) Comprehensive phylogenetic analysis of DA receptors and ADRA1 sequences. The sequences belonging to the D2 cluster of DA receptors (dotted line, yellow background) were not included in this analysis and were added manually to this phylogenetic tree. The tree was constructed using an unweighted pair-group method with arithmetic mean (UPGMA) test. Numbers at the nodes are for the percent supports in 500 bootstrap replicates. (B) Hypothetical evolutionary scenario for InvD1L (magenta) and ADRA1 (green) receptors. Note that divergence of the two receptors likely occurred in the early Bilateralia, while InvD1L was lost in the early Chordata and ADRA1 was lost in Insecta. (C) Table summarizing the synonyms commonly used for different DA receptors of *I. scapularis and D. melanogaster*. GenBank Accession numbers for: ***InvD1L subgroup***: *Anopheles gambiae*, XM_311193.4; *Apis melifera*, NM_001011567.1; *Bombyx mori*, NM_001114866.1; *Branchiostoma floridae*, AM396589.1; *Caenorhabditis elegans*, NM_075837.2; *Capitella teleta* ELU02582.1; *Crassostrea gigas*, JH817851.1; *Daphnia pulex*, GL732531.1; *Drosophila melanogaster* DopR2, NM_001276143.1; *Ixodes scapularis*, XM_002399612.1, *Nasonia vitripennis*, NM_001162377.1; *Pediculus humanus corporis*, XM_002431176.1; *Saccoglossus kowalevskii*, XM_002737161.1; *Strongylocentrotus purpuratus*, XM_003729956.1; *Schistosoma mansoni*, XM_002576487.1, *T. castaneum*, XM_967686.2; **ADRA1 group:** *B. floridae*, XM_002608903.1; *C. teleta*, KB294741.1; C. gigas, EKC41004.1, *D. pulex*, EFX64650.1; Gallus gallus, XM_420871.2; *Homo sapiens* ADRA1D, NM_000678.3; *Metaseiulus occidentalis*, XM_003748355.1; *Oncorhynchus mykiss*, NM_001124675.1; S. *kowalevskii*, XM_002733883.1; *S. purpuratus*, XM_003726189.1; ***D1 subgroup***: *D. melanogaster* DopR, NM_001260163.1; *H. sapiens* D1, X58987.1; *H. sapiens* D5, AY136750.1; *I. scapularis* D1, XM_002409243.1; **D2 cluster:** *D. melanogaster* D2R, NM_001031909.1; *H. sapiens* D2, S62137.1; *H. sapiens* D3, BC095510.1; *H. sapiens* D4, AB065765.1; *I. scapularis* D2, XM_002416405.1

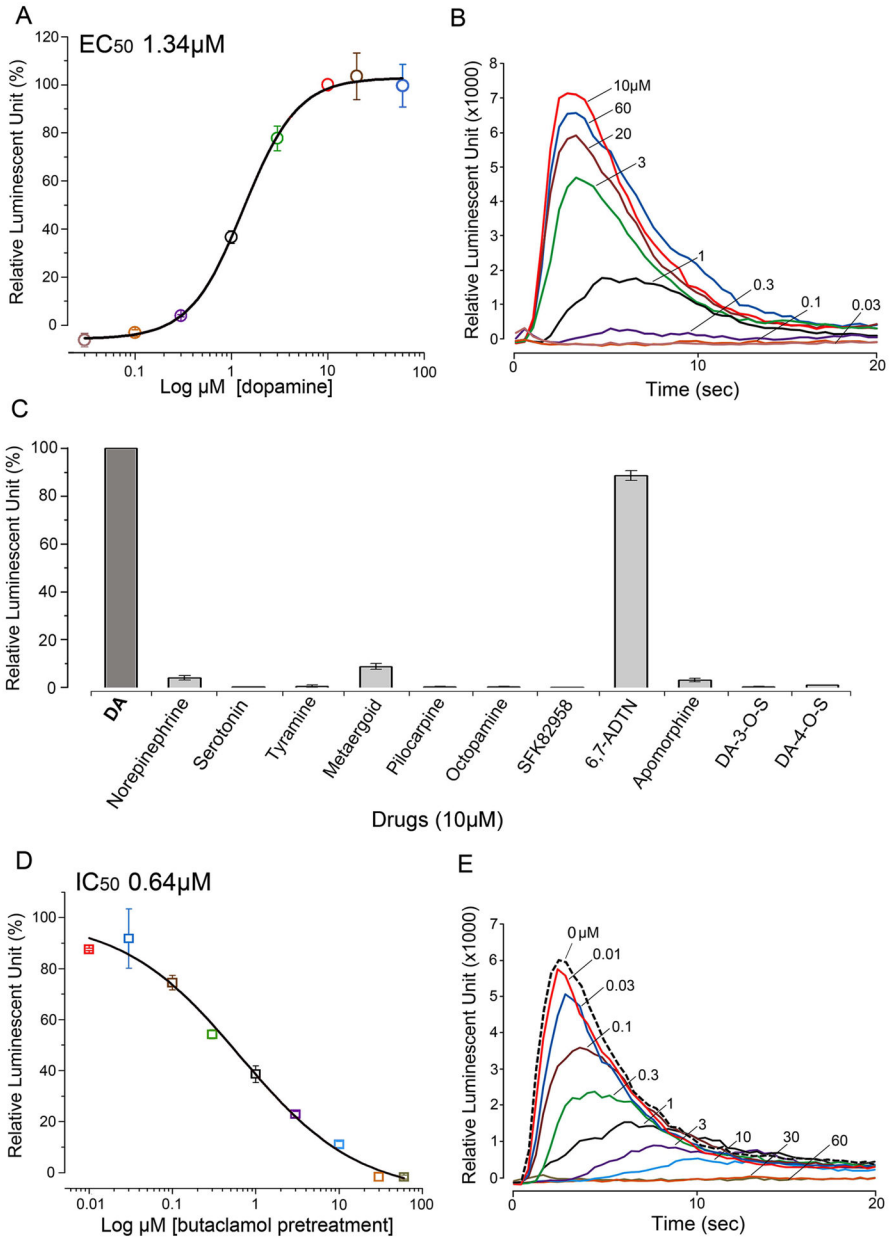

Figure 2.

Bioluminescent aequorin reporter assays for InvD1L receptor expressed in Chinese hamster ovary cells (CHO-K1). (A) Dose-response curve of InvD1L receptor to various doses of dopamine (DA). (B) Representative luminescence responses of InvD1L when treated with different doses of DA (30 nM to 60 μM). (C) Agonistic activities of various chemicals (10 μM) on the InvD1L receptor. (D) Dose-responses curve of the antagonistic activity of (+)butaclamol on the DA-mediated (10 μM) InvD1L receptor activity. (E) Representative luminescence responses of InvD1L to 10 μM DA after pre-incubation with different concentrations of (+)butaclamol for 15 minutes. For details of chemicals used, see section 2.1 Tick samples and chemicals. The colors in A and D correspond to those of the curves in B and E, respectively. The bars in A, C and D indicate the standard error for three replicates.

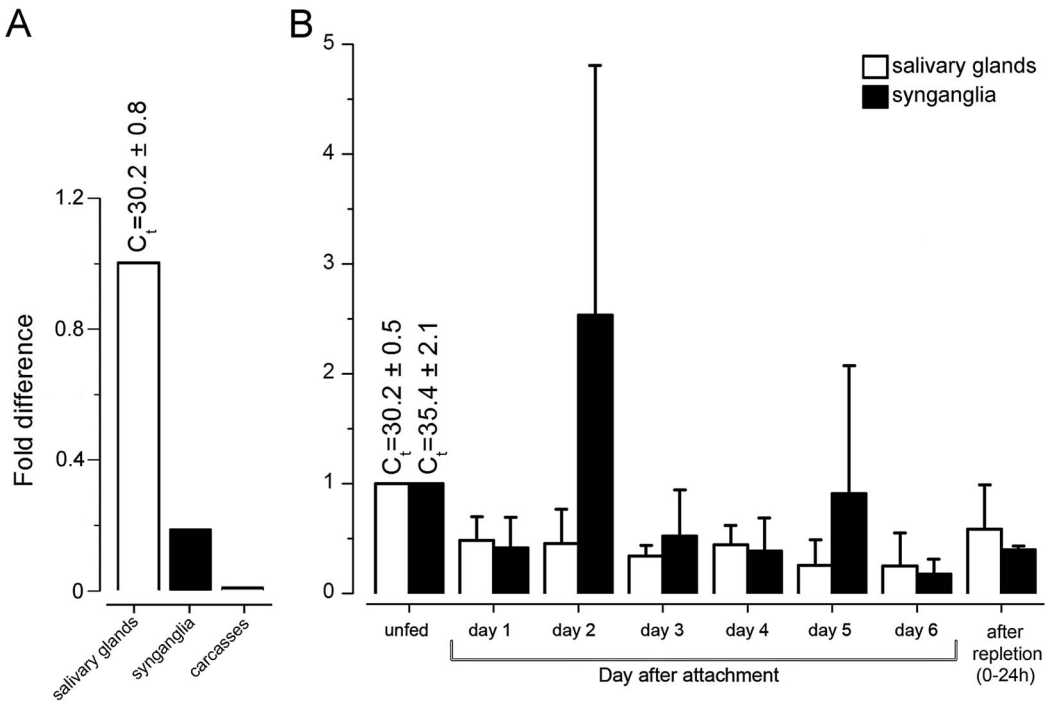

Figure 3.

Tissue-specific (A) and stage-specific (B) levels of *invd1l* transcripts measured by quantitative real-time reverse transcriptase-PCR (qRT-PCR). (A) qRT-PCR showing the transcript levels of *invd1l* receptor in different tissues. Note that the cDNAs were from the pools of tissues in daily collections of unfed, 1–6 day fed, and fully engorged females. (B) Changes in the mRNA levels of *invd1l* in the synganglia (filled bars) and the salivary glands (empty bars) during various feeding phases. The standard deviations for a minimum of three biological replicates are shown in B. The data were normalized using the ribosomal protein S4 (RPS4) transcript, and the highest expression levels were assigned a value of 1. The Ct values (± standard deviation) for the biological replicates are shown. Further experimental details can be found in Section 2.4 Quantitative real-time reverse transcriptase-PCR (qRT-PCR).

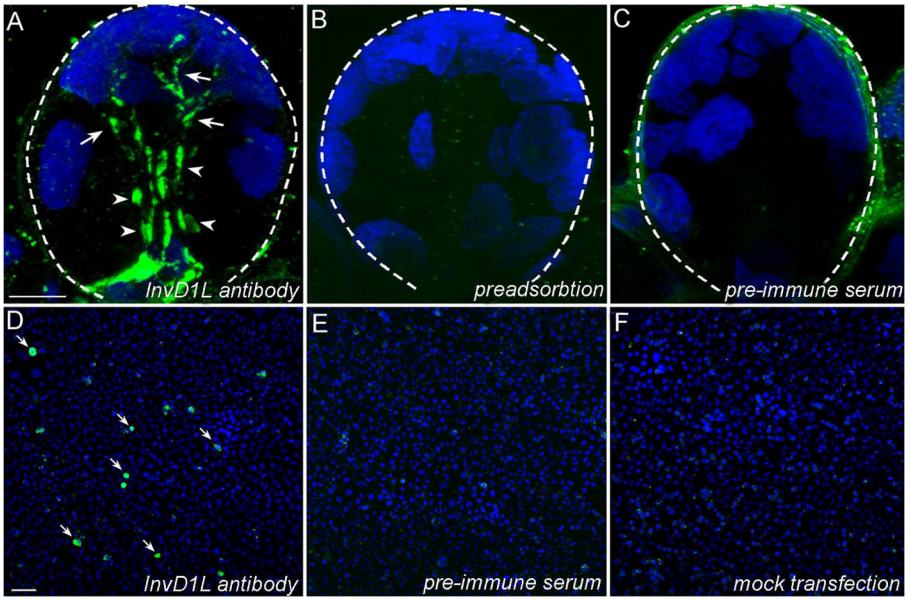

Figure 4.

Characterization of anti-InvD1L antibody in positive and negative controls. (AC) Acinus type III from unfed female. (A) Positive staining for InvD1L receptor. Arrowheads, InvD1L immunoreactive (IR) axon terminals; arrows, InvD1L IR elongated axon-like processes. (B) Preadsorption negative controls for InvD1L receptor staining. InvD1L antibody was pre-incubated with the synthetic antigenic peptide (1 μM) for four hours at room temperature. (C) Pre-immune serum negative controls for InvD1L staining. (D-F) Positive immunoreactivity (IR) and negative controls in immunohistochemistry of InvD1L receptor in Chinese hamster ovary cells (CHO-K1) transfected with *invd1l*. (D) The IR of CHO cells transfected with *invd1l* to anti-InvD1L (green, arrows). (E) The IR of CHO-K1 cells transfected with *invd1l* to pre-immune serum. (F) The IR of mock-transfected CHO-K1 cells to anti-InvD1L. The microscope settings for image capture were identical for the positive and negative controls. Blue color represents DAPI staining for nuclei. Dotted lines in A, B and C show the boundary of an acinus. For more details, see section 2.5, Antibodies and immunohistochemistry. Scale bars = 10 μm in A (applies to A–C); 10μm in D (applies to D–F).

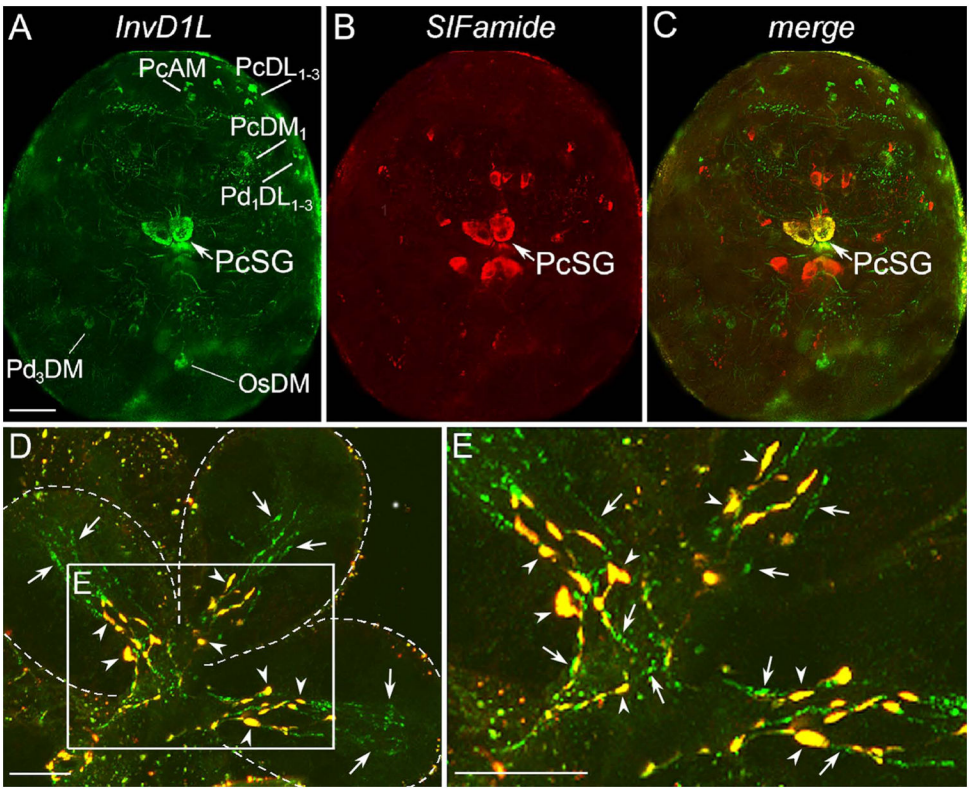

Figure 5.

Immunohistochemistry for InvD1L receptor (green) and SIFamide neuropeptide (red) in double-staining of synganglia and salivary glands (type III acini). Colocalization of both InvD1L and SIFamide is shown in yellow. (A–C) Double-staining of InvD1L receptor (green, A) and SIFamide (red, B) revealed various sets of neurons and their projections in the dorsal view of the synganglion of one-day fed *Ixodes* female. Colocalization (yellow) of InvD1L and SIFamide was detected only in one pair of protocerebral salivary gland neurons (PcSG) in the synganglion. For descriptions of all InvD1L positive neurons detected in this study, see Fig. 6. SIFamide-positive neurons were previously described in Šimo et al., 2009b. For abbreviations of labeled peptidergic neurons, see part 2.6 The nomenclature of peptidergic neurons, or the list of abbreviations. (D) Multiple confocal layers collapsed in one image of type III acini. Two different types of IR for InvD1L are shown: basal axon terminals with colocalization of InvD1L and SIFamide-IR (yellow, arrowheads), and InvD1L receptor IR in longer axon-like processes (green, arrows). (E) Higher magnification of inset in D. Note that both InvD1L/SIFamide (yellow, arrowheads) and InvD1L-only (green, arrows) projections arborize in basally located branches (3–4 or 5–7 branches, respectively). Dotted lines in D show boundaries of individual acini. This figure is repeated as Supporting Information Fig. 1 with the color combinations of magenta-green. Scale bars are 50 μm for A–C and 10 μm for D and E.

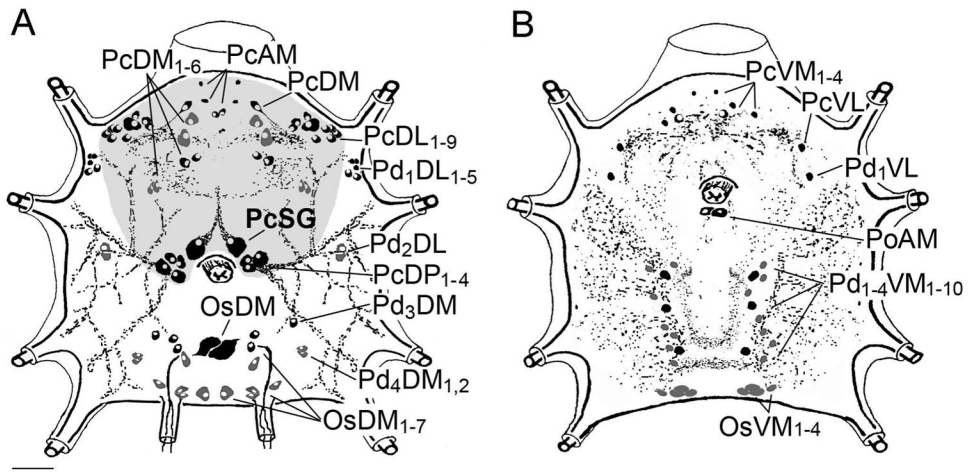

Figure 6.

Schematic diagram showing the neurons and their projections immunoreactive to the antibody for InvD1L receptor. The diagrams are each for (A) dorsal, (B) ventral side of the synganglion in one-day fed female. Grey background in A represents the protocerebrum including its all InvD1L immunoreactive neurons. Neurons in black represent strong immunoreactivity (IR); those in grey represent weak IR. For explanation of the abbreviations of labeled peptidergic neurons, see part 2.6, The nomenclature of peptidergic neurons, or the list of abbreviations. Scale bar, 50 μm.

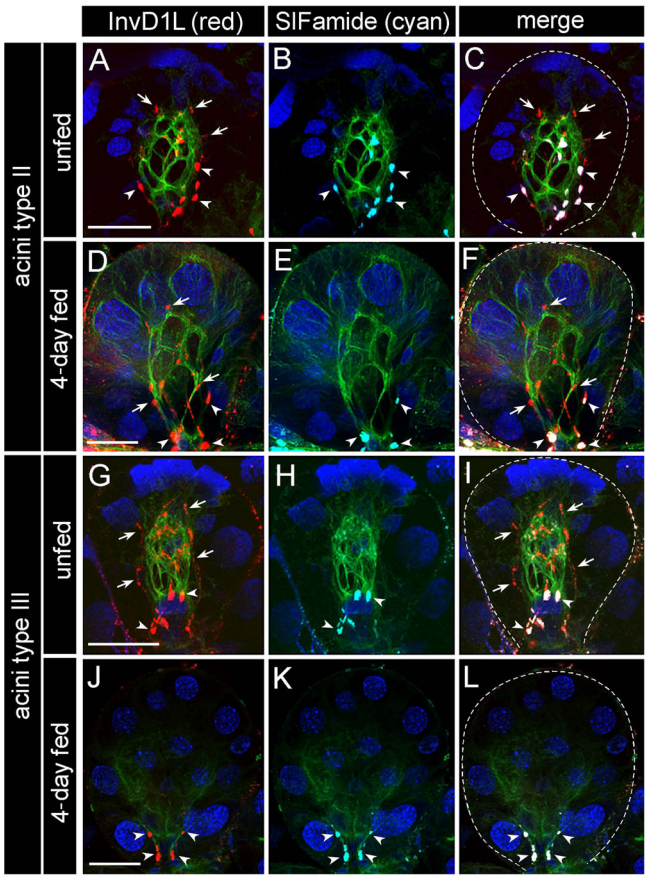

Figure 7.

Immunohistochemistry for InvD1L receptor (red, A, D, G, J), SIFamide neuropeptide (cyan, B, E, H, K) and β-tubulin (green). The basally located axon terminals stained for both InvD1L (red) and SIFamide (cyan) are marked by arrowheads, while the longer axon-like processes IR-positive only for InvD1L receptor (red) are marked by arrows. White color in the merged image (C, F, I, L) indicates colocalization (arrowheads) of InvD1L receptor and SIFamide neuropeptide. Blue color represents DAPI staining for nuclei. Dotted lines in the merged images represent the boundary of an acinus. This figure is repeated as Supporting Information Fig. 2, with color combinations of magenta-green. Scale bar, 20 μm.

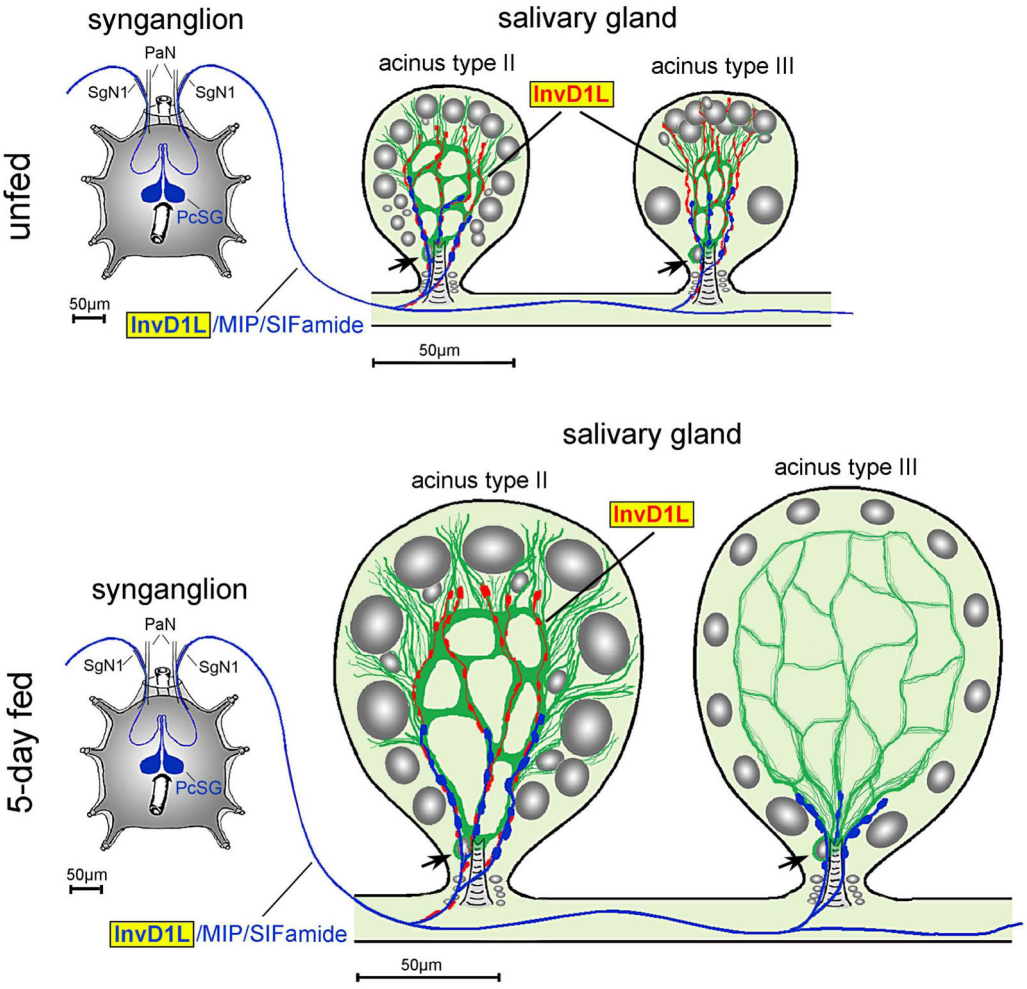

Figure 8.

Schematic diagram showing InvD1L IR in the synganglion and the salivary gland acini, types II and III, of unfed and 5-day fed females. Blue represents colocalization of InvD1L, myoinhibitory peptide (MIP), and SIFamide. Red represents the InvD1L-only IR with longer axon-like processes in the acinus. The InvD1L-IR axon like-processes (red) run along the putative myoepithelial cell (green) close to the acinar lumen, which disappears in the type III acini within the first two days after the initiation of feeding. Grey color in salivary gland acini represents different cell types with nuclei having different sizes. Arrow indicates the nucleus of putative myoepithelial cell. PaN, palpal nerve; SgN1, salivary nerve 1; PcSG, protocerebral salivary gland neurons.

Table 1

Antibodies used in this study.

Antibody name	Host	Dilution	Source/characterization	Immunogen
Ixosc InvD1L	Chicken polyclonal, affinity purified	1:1,000	This study	CRIIKEDASMRSQSLEEAVL
Drome SIFamide	Rabbit polyclonal	1:1,000	Terhzaz et al., 2006	AYRKPPFNGSIFamide
β-tubulin	Mouse monoclonal	1:1,000	GEnScript (2G7D4)	Purified human recombinant full-length